Comparison of NCEP–NCAR Cloud Radiative Forcing Reanalyses with Observations

BRYAN C. WEARE

Atmospheric Science Program, Department of Land, Air and Water Resources, University of California, Davis, Davis, California

(Manuscript received 15 August 1996, in final form 24 February 1997)

ABSTRACT

Longwave and shortwave cloud radiative forcing from the recently released National Center for Environmental Prediction–National Center for Atmospheric Research (NCEP–NCAR) reanalyses are compared to Earth Radiation Budget Experiment (ERBE) observations. The observed differences are analyzed utilizing concurrent International Satellite Cloud Climatology Project (ISCCP) estimates of cloudiness and other satellite observations.

The results show that the NCEP–NCAR longwave cloud forcing agrees well with that of ERBE not only for the annual means but also for seasonal and climatic variations. Areas of disagreement are generally related to disagreements between NCEP–NCAR high cloudiness and observations. Overall, the NCEP–NCAR shortwave cloud forcing is in poorer agreement with ERBE observations. NCEP–NCAR annual means in the Tropics are often 20–30 W m^{-2} too negative. On the other hand the NCEP–NCAR total cloud cover in this region is 10%–20% less than the ISCCP observations, which should lead to less, rather than more, negative shortwave cloud forcing. Thus the primary error in the mean shortwave cloud forcing is likely due to specification of clouds that are too reflective in the NCEP analysis model. Moderate errors in the variability of NCEP–NCAR SWCF are apparently related to errors in the analyzed seasonal variability of total cloudiness, which are exacerbated by NCEP model specification of clouds that are too bright and underestimates of the seasonal variability of the clear-sky fluxes.

1. Introduction

Recently the first results of the reanalysis undertaken by the National Centers for Environmental Prediction (NCEP formally known as the National Meteorological Center, NMC) and the National Center for Atmospheric Research (NCAR) have been described (Kalnay et al. 1996). This reanalysis is the result of a tremendous effort to develop a high quality homogeneous dataset of most relevant atmospheric variables over the period of modern observations. Monthly means of the analyses are currently available for the period January 1982 through December 1994 on the ''AMS CD-ROM,'' distributed with the above article. Each of the many available variables has been given a designation ''A,'' ''B,'' or ''C,'' corresponding to variables that are strongly influenced by observations, influenced by both observations and the analysis model, and solely from model output forced by data assimilation, respectively. A large fraction of the ''C'' variables are radiative terms at both the top of the atmosphere and the surface. Since radiative feedbacks are thought to be critical for past and future climate changes (Houghton et al. 1996), it seems essential to thoroughly evaluate the utility of the NCEP–NCAR analyses of these radiative variables. This paper makes comparisons with Earth Radiation Budget Experiment (ERBE) observations of the annual means, seasonal cycles, and a short-term climate change event for the long- and shortwave radiative cloud forcing at the top of the atmosphere.

To evaluate not only whether the NCEP–NCAR analyses of cloud radiative forcing are in agreement with observations, but to also understand the nature of any disagreements, it is necessary to comprehend what controls mean cloud radiative forcing and its variations. Cloud radiative forcing for longwave radiation at the top of the atmosphere may be defined by

$$\mathrm{LWCF} = E_{\mathrm{clr}} - E \approx f_{\mathrm{high}}(E_{\mathrm{clr}} - E_{\mathrm{high}}), \qquad (1)$$

where E is the longwave total scene radiative flux. Here, E_{clr} and E_{cld} are the corresponding radiative fluxes for completely clear and cloudy skies, and f_{high} is the fraction of sky covered by cloud. A basic assumption in interpreting cloud radiative forcing is that E_{clr}, whose variations are mainly a function of surface temperature and precipitable water, changes slowly over relatively large scales so that variations in LWCF over space and time are primarily related to changes in cloud amount and properties. Ramanthan et al. (1989) argue that spatial variations of the mean longwave cloud radiative forcing are primarily related to the variations in high, optically thick cloud amounts as indicated by the last expression in Eq. (1). Because clouds tend to be colder than the

Corresponding author address: Prof. Bryan C. Weare, Atmospheric Science Program, Department of Land, Air and Water Resources, University of California, Davis, Davis, CA 95616.
E-mail: bcweare@ucdavis.edu

surface, variations in longwave cloud radiative forcing are nearly always positively related to those in high cloud amounts.

Cloud radiative forcing for shortwave radiation at the top of the atmosphere may be defined by

$$\mathrm{SWCF} = S_{\mathrm{clr}} - S = f(S_{\mathrm{clr}} - S_{\mathrm{cld}}), \qquad (2)$$

where S is the shortwave total scene reflected flux, f is the total cloud cover, and S_{clr} and S_{cld} are the corresponding reflected fluxes for completely clear and cloudy skies. The geographic variations in S_{clr} are primarily related to variations in downward solar radiation at the top of the atmosphere, surface albedo, and precipitable water. Those in S_{cld} are in addition mainly functions of total cloud water and cloud drop size. Since clouds are usually more reflective than the surface, except perhaps snow and ice, shortwave cloud radiative forcing variations are negatively related to variations in f.

Weare (1995a, 1997) has investigated the relationships between seasonal and interannual variations in ERBE cloud radiative forcing and possible forcing terms derived from International Satellite Cloud Climatology Project (ISCCP) low, middle, and high cloud observations and operational analyses of temperature and moisture. Longwave cloud forcing is shown to be strongly related to high cloud amounts at all latitudes and also to E_{clr} at high latitudes. The contributions of low and middle cloud cover, cloud water path, and upper-tropospheric temperature are smaller and relatively independent of latitude. The situation for shortwave cloud forcing is somewhat more complex. The most important factor related to its variability is high cloud cover, followed closely by cloud water path and clear-sky albedo at high latitudes. Middle and low cloud cover also make substantial contributions.

The current analysis will rely upon this basic understanding of cloud radiative forcing to develop better insight into the reasons for any significant differences between NCEP–NCAR cloud radiative forcings and ERBE observations. Thus, NCEP–NCAR cloud radiative forcing errors are related to the pattern of the differences between observations and NCEP–NCAR reanalyses of high and total cloud cover, clear-sky fluxes, and atmospheric humidity. Unfortunately, cloud optical depth is not available in the current NCEP–NCAR reanalysis product.

2. Analyses and observations

Monthly ERBS longwave and shortwave clear-sky and total fluxes equatorward of about 60° are available on a 2.5° grid for the four years 1985–88. Data from this single satellite are chosen because they are the result of relatively uniform sampling of the diurnal cycle, and because they are thought to have fewer systematic errors than the combined ERBE three-satellite data (Potter 1994, personal communication). In these observations the total scene fluxes are carefully derived from full spectrum scanning radiometer observations. The ERBS clear-sky fluxes are means of the subsets of those observations that are judged to be clear (Diekmann and Smith 1989). Several authors suggest that there may be biases in these clear-sky fluxes of up to 10 W m^{-2} (e.g., Harrison et al. 1990; Hartmann and Doelling 1991).

The NCEP–NCAR reanalysis provides for January 1982 through December 1994 monthly means of total and clear-sky fluxes of outgoing longwave and reflected shortwave radiation at the top of the atmosphere. In the NCEP–NCAR analyses both sets of fluxes are derived from a radiative transfer model driven by various inputs, including temperature, moisture, and cloud amount. The radiative transfer model is a component of the NCEP analysis forecast model, which is very similar to the ''NMC'' model, which was a participant in the Atmospheric Model Intercomparison Project (AMIP; Gates 1992). In this model, cloud amount is derived from a diagnostic scheme and radiative properties are simple functions of temperature and height (Phillips 1996, 1994). Unlike in the ERBE observations the clear-sky fluxes are derived at all locations and times as the radiative fluxes that are calculated when cloud amounts are set to zero, but all other properties of the atmosphere are those of the total sky calculation. Cess et al. (1992) discuss the generally small differences that arise among the different methods for calculating cloud radiative forcing. The comparisons illustrated below are for the region 60°S–60°N for the four years January 1985–December 1988.

The ISCCP C2 (Rossow and Schiffer 1991) monthly fractions for total f and high f_{high} cloud cover were obtained from NCAR. High cloud amounts are defined as the fraction of clouded pixels that have emission temperatures corresponding to pressures less than 440 hPa relative to the total number of pixels in a region. The ISCCP cloud data have been chosen as the primary comparison variable because they provide the best available multiyear global cloud analyses. Rossow and Schiffer (1991), Fu et al. (1990), and Weare (1993, 1994) provide evidence that ISCCP variables, such as total cloud cover, visible optical depth, and cloud-top pressure, at least qualitatively mimic important aspects of large-scale monthly averages. In addition ISCCP high cloud observations have been compared with the very sensitive, but relatively infrequent, *SAGE II* satellite measurements (Liao et al. 1995) and with ground-based lidar measurements (Minnis et al. 1993). These comparisons show generally good agreement, but also suggest that the ISCCP mean high amounts underestimate the true value by approximately one-third.

The AMS CD-ROM provides NCEP–NCAR cloud fractions for the low, middle, and high layers corresponding approximately to the ISCCP pressure level designations. However, a ''reanalysis–problems'' bulletin (www.cdc.noaa.gov/cdc/reanalysis/problems.shtml) dated 12 April 1996 states that the distributed cloud fractions are not those utilized by the NCEP model

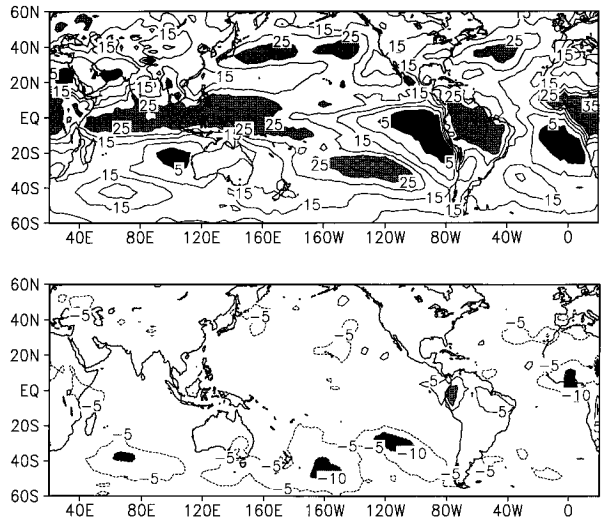

FIG. 1. Annual mean NCEP high cloudiness f_{high} (percent): (a) 1968 ''corrected'' amounts (dark shading: values less than 5%; light shading: values greater than 25%) and (b) 1988 ''uncorrected'' minus 1968 ''corrected'' (dark shading: values less than −10%; light shading: values greater than 10%).

radiation codes because of problems related to the combining of clouds arising separately from convective and large-scale processes. This document states that total cloud may be calculated from the distributed values using the random overlap assumption but that the individual high, middle, and low cloud amounts are ''useless.''

The value of the NCEP–NCAR high cloud amounts was explored utilizing the recently released NCEP reanalyses for 1968, which is the first year in which the high cloud amounts have been corrected (W. Ebisuzaki 1997, personal communication). Since corrected amounts are now available for only one year, a thorough assessment of the errors in the 1982–94 high clouds is impossible. However, as a preliminary assessment the annual mean high cloud amounts for the ''correct'' data in 1968 were compared with the annual means of the ''incorrect'' data for each of the years 1982–94. Figure 1a illustrates the 1968 annual mean cloud cover. The well-known maxima over the tropical convective zones and minima over the subtropical highs are very evident. Figure 1b illustrates the ''incorrect'' 1986 annual means minus those for 1968 (Fig. 1a). 1986 is approximately ''equivalent'' to 1968 in that both precede a moderate El Niño–Southern Oscillation event. In general, the ''incorrect'' 1986 amounts are a few percent cloud cover less than those for 1968 everywhere except over the Amazon region. However, large areas of differences of more than 5% cloud cover are only evident south of about 30°S, an area in which a number of differences between the two analyses are likely to exist, in part because of differences in available satellite data for the two periods. Except for El Niño years, other difference maps (not shown) are very similar to Fig 1b. The three El Niño years have in the eastern Pacific region the expected greater high cloud amounts of between 5% and 10%. Based on this and other comparisons of NCEP–NCAR, AMIP NMC, and C2 values (Weare et al. 1996), it appears that although instantaneous values of f_{high} may be questionable, as stated in the ''reanalysis–problems'' bulletin, north of about 30°S, especially over the oceans, monthly means of f_{high} in the 1982–94 NCEP reanalysis high clouds mimic the mean spatial patterns of the true NCEP model high cloud. Thus 1982–94 NCEP–NCAR f_{high} will be utilized with care in the remaining parts of this paper.

In addition to these primary data, several other related datasets have been analyzed. These include net downward solar radiation at the surface (Li and Leighton 1993), Special Sensor Microwave/Imager (SSM/I) atmospheric precipitable water (Greenwald et al. 1993), and TIROS Operational Vertical Sounder (TOVS) Pathfinder A cloud amounts (Susskind et al. 1997).

The surface net downward solar radiation S_{surf} was derived from a physical model using ERBE observations. The spatial pattern of this quantity depends upon the extraterrestrial input, which is reduced by cloud reflection, and absorption, primarily by water vapor and stratospheric ozone. This is described approximately by the equation

$$S_{surf} = S_0 \mu T_{clr}(1 - fr_{cld})(1 - r_s), \qquad (3)$$

where S_0 is the solar flux at the top of the atmosphere; μ is the cosine of the solar zenith angle; T_{clr} is the transmissivity of a clear atmosphere, whose variations are primarily a function of those in precipitable water; f is the total cloud cover; r_{cld} is the cloud reflectivity, whose variations are primarily a function of cloud water content and droplet size; and r_s is the surface albedo. These data were obtained from the Canadian Environmental Monitoring Service World Wide Web site for the period of the ERBS observations.

The TOVS Pathfinder A cloud amounts are the emissivity weighted cloud amounts, which are the products of the sophisticated retrieval of temperature, moisture, and ozone from relatively coarse resolution infrared and microwave sounding radiometers. They were obtained over the Internet from the NASA's Distributed Active Archive Center (DAAC) for the ERBS period. Comparisons were made between the ISCCP and TOVS cloud amounts. They show excellent agreement for high clouds for both the annual means and the amplitudes and patterns of the seasonal cycle. However, for total cloud cover the TOVS analysis has far fewer clouds, especially over ocean where ISCCP values exceed those of TOVS by 10%–30%. This is apparently due to the fact that the TOVS analysis strongly underestimates the numbers of oceanic middle and low clouds (Susskind et al. 1997; Wielicki and Coakley 1981).

The SSM/I precipitable water, which is also available at the NASA DAAC site, is available only over ocean and without gaps during only the last 2 yr of the ERBS

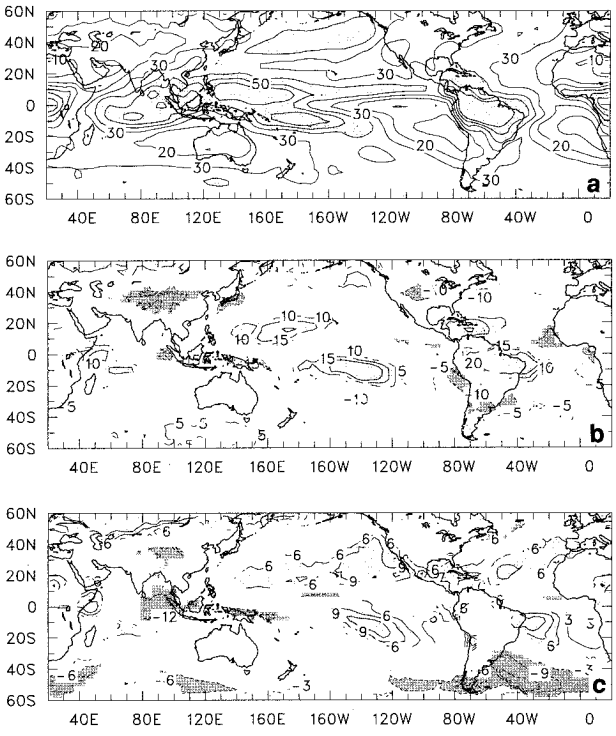

FIG. 2. Annual mean statistics based upon data for January 1985 through December 1988: (a) NCEP–NCAR annual mean longwave cloud forcing (W m^{-2}), (b) NCEP–NCAR minus ERBE annual mean longwave cloud forcing (W m^{-2}), and (c) NCEP–NCAR minus ISCCP annual mean high cloud amount (percent). In (b) and (c) only differences that are significantly different from zero at the 95% confidence level are plotted.

data. Ferraro et al. (1996) argue that precipitable water is the most accurately inferred variable from SSM/I observations with errors of about 10%.

The following comparisons are made for both long- and shortwave cloud radiative forcing and related variables, using maps of the annual means, the seasonal cycle (defined by departures from the annual means), and differences between August of the La Niña year 1988 and the El Niño year 1987. The choice of these latter times corresponds to those of displayed maps of other variables in Kalnay et al. (1996).

The 95% significance levels of the results are assessed using Student's t-test statistics for the means and E statistics for the ratios of the standard deviations of departures from the annual means (Brunk 1965). The effective number of degrees of freedom N_{eff} was determined following the analysis of Weare (1994) of ISCCP cloud fractions in which it was concluded that N_{eff} is no less than one-half the number of monthly time samples. Thus, in this study N_{eff} is set everywhere to half of the total number of months of data.

3. Annual means

Figure 2 shows the annual mean NCEP–NCAR longwave cloud radiative forcing, the difference between the NCEP–NCAR and ERBS means, and the difference between the annual mean NCEP–NCAR and ISCCP high cloud fractions. The annual mean longwave cloud forcing (Fig. 2a) is qualitatively very similar to the ERBS mean (not shown). The largest differences are in the Tropics such that the NCEP–NCAR values are often up to about 15 W m^{-2} larger than the ERBE. Only in small, relatively scattered regions are the NCEP–NCAR means significantly smaller than the ERBE values. The regions in which the NCEP–NCAR values significantly differ from the observations often correspond approximately to those regions in which the NCEP–NCAR f_{high}'s significantly depart from the ISCCP values (Fig. 2c). However, one must keep in mind that the ISCCP estimates of high cloud amounts are likely underestimates of the ''true'' high cloud amounts and that there are uncertainties in the 1982–94 NCEP–NCAR f_{high}. The latter may help explain the relatively poor agreement between the errors in LWCF and f_{high} in the higher latitudes of the Southern Hemisphere. Difference maps (not shown) between NCEP–NCAR and TOVS high clouds are nearly identical to Fig. 2c. Using Eq. (1), Fig. 2 suggests that the moderate errors in the NCEP/NCAR mean longwave cloud forcing are primarily the result of errors in the specification of the regional pattern of high cloud amounts in the NCEP analysis model.

An alternate explanation for the discrepancies between the NCEP–NCAR and ERBE cloud radiative forcing values might be that they are primarily due to differences in the NCEP–NCAR and ERBE clear-sky fluxes E_{clr}. Several papers (e.g., Potter et al. 1992: Cess et al. 1992) have investigated the possible differences in E_{clr} that arise from the different methods used to calculate the ERBE and model clear-sky fluxes. A comparison (not shown) of annual mean E_{clr} indicates that over ocean the ERBE and NCEP–NCAR values differ nearly everywhere by less than 5 W m^{-2}, less than the differences illustrated in Fig. 2b. However, larger differences of up to about 15 W m^{-2} are evident over a number of land areas including the Himalayan plateau. Thus, most of the differences illustrated in Fig. 2b, particularly those over the oceans, are unlikely to be attributable to differences in the clear-sky fluxes.

Figure 3 shows the annual mean shortwave NCEP–NCAR cloud radiative forcing, the difference from ERBS, and the difference between the NCEP–NCAR annual mean total cloud amount and the ISCCP values. The NCEP–NCAR cloud radiative forcing is up to about 50 W m^{-2} less than the ERBS values over nearly all of the Tropics and subtropics. Since ERBE shortwave cloud forcing in this region is generally between -20 and -70 W m^{-2} (not shown), this implies errors are in the range of the observed magnitudes. The SWCF difference pattern is not well related to the pattern of the differences between NCEP–NCAR and ISCCP total cloud in which the differences are generally largest in the middle, rather than tropical, latitudes. Furthermore, contrary to what is expected from Eq. (2), the negative

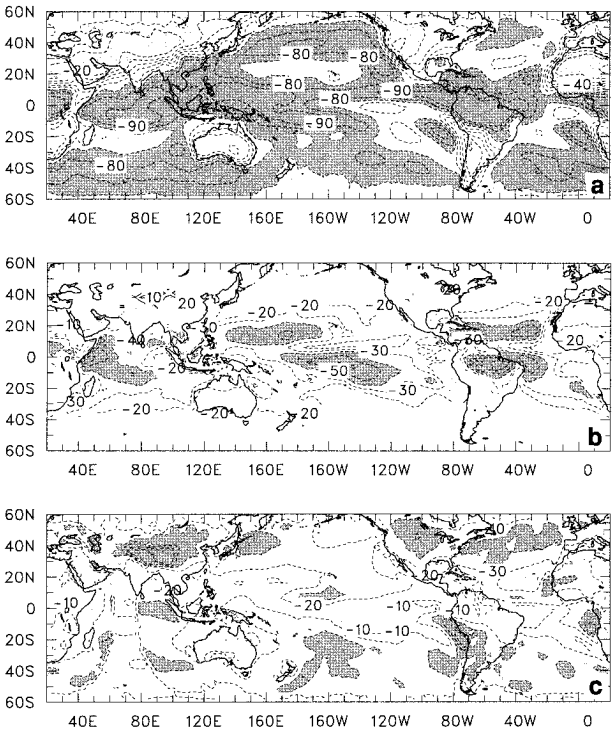

FIG. 3. (a) NCEP–NCAR annual mean shortwave cloud forcing (W m^{-2}), (b) NCEP–NCAR minus ERBE annual mean shortwave cloud forcing (W m^{-2}), and (c) NCEP–NCAR minus ISCCP annual mean total cloud amount (percent). In (b) and (c) only differences that are significantly different from zero at the 95% confidence level are plotted.

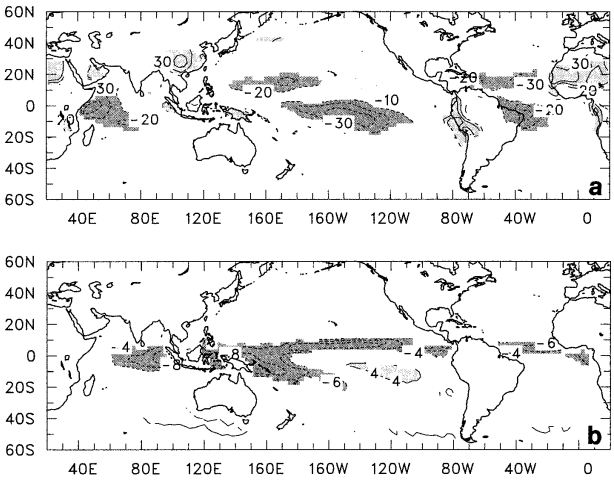

FIG. 4. (a) NCEP/NCAR minus Li and Leighton annual mean net surface downward solar flux (W m^{-2}), and (b) NCEP–NCAR minus SSM/I annual mean total precipitable water (kg m^{-2}). Only differences that are significantly different from zero at the 95% confidence level are plotted.

SWCF differences are broadly related to negative, rather than positive, e differences.

Again, the differences between the NCEP–NCAR and ERBE shortwave cloud forcing estimates could be related to differences in the respective clear-sky fluxes. However, over ocean the differences between the annual means of the NCEP–NCAR and ERBE clear-sky reflected shortwave fluxes (not shown) are less than 5 W m^{-2}. The only exception is a narrow band along the equator where the NCEP–NCAR values exceed those of ERBE by slightly more than 5 W m^{-2}. However, from Eq. (2) this should result in less negative NCEP–NCAR shortwave cloud forcing rather than the more negative values illustrated in Fig. 3b. Over land, especially at higher latitudes, differences between the NCEP–NCAR and ERBE annual means often exceed 10 W m^{-2}. However, these differences do not appear to contribute to large differences in shortwave cloud forcing.

Figure 4 illustrates two other related analyses. The differences between the net downward shortwave radiation at the surface S_{surf} from the NCEP–NCAR analysis and from observations (Li and Leighton 1993) are shown in Fig. 4a. This figure shows significant differences centered on the areas of maximum SWCF differences over a limited sector of the oceanic subtropics. From Eq. (3) longitudinal differences in net downward shortwave radiation at the surface may largely be attributed to differences in water vapor absorption, total cloud cover, and/or cloud reflectivity. The pattern of probable errors in the NCEP–NCAR analysis of water vapor absorptivity can be inferred from Fig. 4b, showing the differences between NCEP–NCAR annual mean total precipitable water and values inferred from the SSM/I observations. A comparison of the difference patterns in Fig. 3b and 4a and that of Fig. 4b show that the errors in SWCF and S_{surf} are not well related to errors in vertically integrated water vapor amount in the NCEP–NCAR analysis. In fact, Fig. 4b shows errors in precipitable water in the equatorial oceans are associated with minimum errors in S_{surf}. The pattern of the differences in total cloud cover between NCEP–NCAR and ISCCP (Fig. 3c) does not correspond well to that of Fig. 4a.

4. Seasonal cycle

Figure 5 shows the spatial patterns of the most important empirical orthogonal functions (EOFs) of departures of the longwave cloud forcing from the annual means for the NCEP–NCAR analysis and ERBS observations. These dominant EOFs both pass the commonly employed test for significance at the 95% confidence level suggested by North et al. (1982). The time coefficients (not shown) both have a strong seasonal cycle with very similar magnitudes and phases such that maxima exist in July/August and minima in January/February. The spatial patterns are also very similar, suggesting that the NCEP–NCAR reanalysis expresses well the larger-scale features of the seasonal cycle of longwave cloud forcing. Differences, however, do exist.

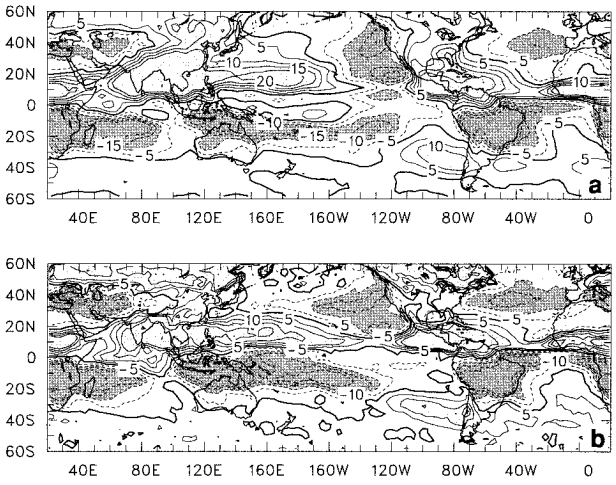

FIG. 5. Spatial weights of the dominant empirical orthogonal functions of January 1985–December 1988 departures from the annual means of longwave cloud forcing from (a) the NCEP–NCAR reanalysis, explaining 46% of the variance, and (b) the ERBE observations, explaining 35% of the variance.

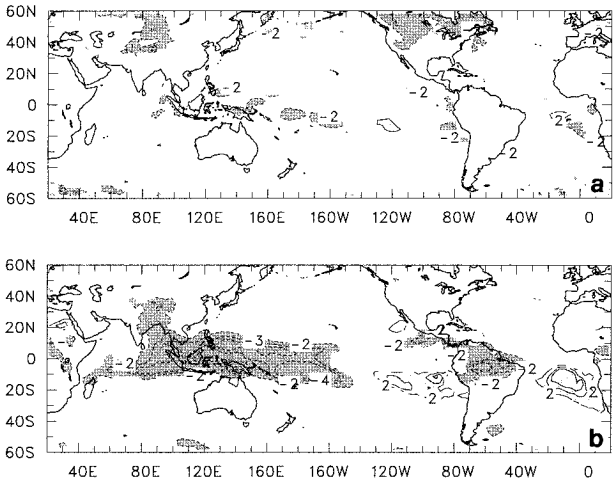

FIG. 6. Seasonal cycle statistics based upon departures from annual means for January 1985–December 1988: (a) ratios of the standard deviation of longwave cloud forcing from the NCEP–NCAR analysis relative to that of the ERBE observations and (b) ratios of the standard deviation of high cloud cover from the NCEP–NCAR analysis relative to that of the ISCCP observations. Only ratios that are significantly different from one at the 95% confidence level are plotted: negative values imply NCEP–NCAR standard deviations are less than those of the observations.

These are highlighted in Fig. 6a, which shows the ratio of the standard deviations of the seasonal cycle of longwave cloud forcing in the NCEP–NCAR analysis relative to that in the ERBS observations. The largest regions of significant differences are in Middle Asia and Canada and in portions of the equatorial zone in which in nearly all cases the NCEP–NCAR analysis shows a smaller variability than the ERBS observations. The ratio of the standard deviations of the NCEP–NCAR and ISCCP high cloud seasonal standard deviations (Fig. 6b) indicates in the Tropics a modest relationship between the underestimated high cloud variances in the NCEP–NCAR analysis and those in longwave cloud forcing. Ratios using TOVS high cloud amounts (not shown) are very similar to those in Fig. 6b. The comparable ratios for the clear-sky longwave fluxes at the top of the atmosphere (not shown) indicates only small, isolated regions of significant differences. Thus, the important differences in the Tropics between the seasonal variability of the NCEP–NCAR and ERBE LWCF are primarily related to differences from observations of f_{high}; those over the Northern Hemisphere continents are of uncertain origin.

Figure 7 shows the spatial patterns of the most important empirical orthogonal functions of departures of the NCEP–NCAR and ERBS shortwave cloud forcing from their annual means. These spatial patterns are quite different from those obtained from a comparable EOF analysis of the incoming solar radiation at the top of the atmosphere. In the latter case (not shown) the contours are strictly zonal and the zero line is at 23.5° north or south, not near the equator as in Fig. 7. As in the case of the LWCF, the time coefficients (not shown) both have a strong seasonal cycle with phases such that maxima exist in May/June and minima in December. However, the amplitude of the NCEP–NCAR SWCF time coefficients is about 16% larger than that of the ERBS coefficients. This is despite the fact that the amplitude of NCEP–NCAR total cloud cover variations are about 25% smaller than exhibited by the ISCCP observations (not shown).

The spatial patterns of the EOFs are quite similar, suggesting that the NCEP–NCAR reanalysis expresses well the pattern of the seasonal cycle of shortwave cloud forcing. The significant differences are highlighted in

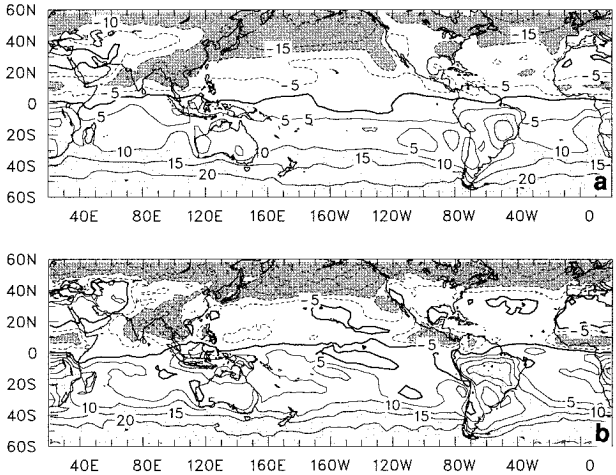

FIG. 7. Spatial weights of the dominant empirical orthogonal functions of January 1985–December 1988 departures from the annual means of shortwave cloud forcing from (a) the NCEP–NCAR reanalysis, explaining 58% of the variance, and (b) the ERBE observations, explaining 29% of the variance.

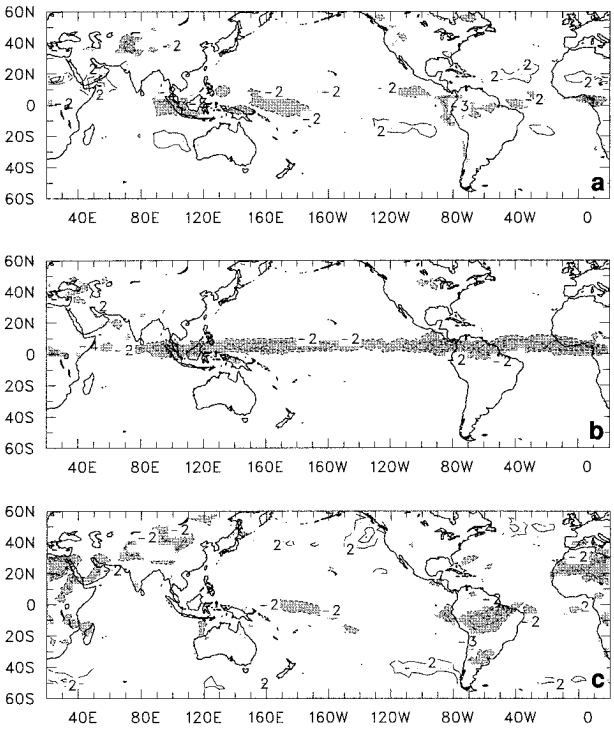

FIG. 8. Seasonal cycle statistics based upon departures from annual means for January 1985 through December 1988: (a) ratios of the standard deviation of shortwave cloud forcing from the NCEP–NCAR analysis relative to that of the ERBE observations, (b) ratios of the standard deviation of clear-sky shortwave fluxes from the NCEP–NCAR analysis relative to that of the ERBE observations, and (c) ratios of the standard deviation of total cloud cover from the NCEP–NCAR analysis relative to that of the ISCCP observations. Only ratios that are significantly different from one at the 95% confidence level are plotted; negative values imply NCEP–NCAR standard deviations are less than those of the observations.

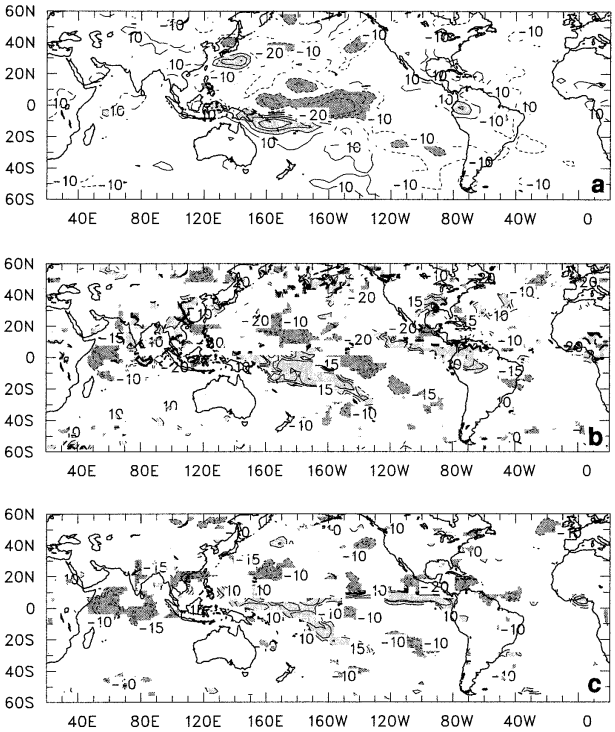

FIG. 9. Differences between values for August 1988 minus those for August 1987: (a) NCEP–NCAR longwave cloud forcing (W m^{-2}), (b) NCEP/NCAR differences minus the ERBE longwave cloud forcing differences (W m^{-2}), and (c) NCEP–NCAR high cloud amount differences minus the ISCCP differences (percent). In (b) and (c) only differences that are significantly different from zero at the 95% confidence level are plotted.

Fig. 8a, showing the ratio of the standard deviations of the seasonal cycles. In general, the significant differences are in the low latitudes such that the NCEP–NCAR reanalysis shows in some locations larger and in other locations smaller variances than the ERBE observations. The overall excessive NCEP–NCAR SWCF variability indicated by the EOF analysis does not represent at individual points over most of the globe a difference that is pointwise significant at the 95% confidence level.

Figures 8b and 8c show that the pattern of errors in NCEP–NCAR SWCF seasonal variability is possibly related to errors in the variability of both clear-sky shortwave fluxes and total cloud amount. However, a comparison of Fig. 8a and 6b suggests that there is a stronger relationship between errors in the amplitude of the seasonal cycle in SWCF and those in f_{high}. Thus, underestimated (overestimated) seasonal variability in the NCEP/NCAR analysis is often related to underestimates (overestimates) of the variability of high clouds. In addition, however, the overall 16% overestimate of NCEP–NCAR SWCF variability observed in the EOF analysis is most likely due to the fact that the NCEP–NCAR clouds are too responsive to seasonal changes in cloudiness.

5. Interannual departures

Figure 9a shows the NCEP/NCAR longwave cloud radiative forcing difference for August 1988 minus August 1987. This figure shows a southwestward shift in cloudiness near the equator in the tropical Pacific Ocean associated with the shift from El Niño to La Niña. Figure 9b shows the difference illustrated in Fig. 9a minus the comparable difference using the ERBS data. In the equatorial central Pacific the NCEP–NCAR analysis shifts the cloudiness too far southward resulting in positive (negative) LWCF differences south (north) of the equator rather than primarily east/west along the equator as in observed cloud changes (Weare 1995b: Weare et al. 1995). The equatorial differences are quite well related to the differences in high cloud cover for August 1988 minus August 1987 between the NCEP–NCAR and ISCCP data (Fig. 9c). In general, the NCEP–NCAR reanalysis appears to qualitatively capture, but improperly locate the interannual departures in high cloud

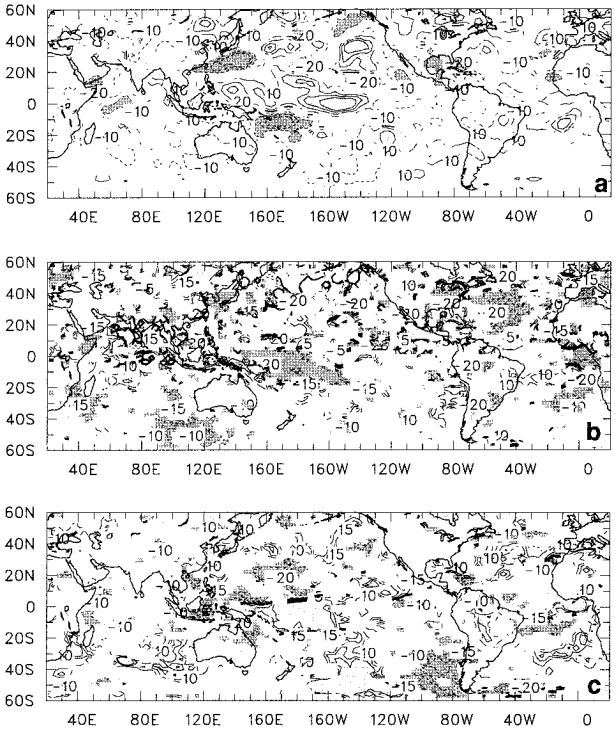

FIG. 10. Differences between values for August 1988 minus those for August 1987: (a) NCEP–NCAR shortwave cloud forcing (W m^{-2}), (b) NCEP/NCAR differences minus the ERBE shortwave cloud forcing differences (W m^{-2}), and (c) NCEP–NCAR total cloud amount differences minus the ISCCP differences (percent). In (b) and (c) only differences that are significantly different from zero at the 95% confidence level are plotted.

amount. This directly contributes to the errors in longwave cloud radiative forcing departures.

The NCEP–NCAR August 1988 minus 1987 shortwave cloud forcing is illustrated in Fig. 10a. As expected, these differences are similar in pattern but opposite in sign to those for LWCF (Fig. 9a). In the equatorial Pacific the disparities between the SWCF differences in the NCEP–NCAR and ERBE results (Fig. 10b) are also similar to the corresponding differences for LWCF (Fig. 9b) with the signs reversed. Also these differences are reasonably well related to differences in total cloud cover between the NCEP–NCAR analysis and ISCCP estimates (Fig. 10c). However, the relatively large differences in cloudiness in the southern Pacific Ocean are not well represented in the SWCF differences. Nevertheless, Fig. 10 suggests that, at least in the Tropics, the patterns of the errors in the NCEP–NCAR shortwave cloud forcing are primarily related to errors in total cloud amount.

6. Discussion

The recently released NCEP–NCAR reanalyses of longwave and shortwave cloud radiative forcing have been compared to ERBS observations. In addition, concurrent ERBS clear-sky fluxes. ISCCP and TOVS observations of cloudiness, and SSM/I precipitable water have been related to the comparable NCEP–NCAR analyses. Comparisons included the annual means, the mean seasonal cycles, and differences between August of the El Niño year 1987 and August of the La Niña year 1988.

These comparisons show generally good agreement between the NCEP–NCAR longwave cloud forcing means and those of ERBS. Areas of disagreement are primarily related to areas of disagreement between NCEP–NCAR high cloudiness and the satellite observational estimates. Overall, the NCEP–NCAR shortwave cloud forcing is in poorer agreement with ERBS observations. The annual means in the Tropics are often too strongly negative by 20–30 W m^{-2}. On the other hand, the NCEP–NCAR total cloud cover in this region has amounts that are 10%–20% less than the ISCCP observations, which should lead to an underestimate rather than the observed overestimate of shortwave cloud forcing.

Kalnay et al. (1996) show that the annual global means of NCEP–NCAR downward shortwave and upward longwave radiation at the top of the atmosphere are in good agreement with observations. They also indicate that the NCEP–NCAR values of top-of-atmosphere upward shortwave are about 11 W m^{-2} greater than the observations, which is consistent with the present results. This overestimate of upward shortwave results in a radiative imbalance at the top of the atmosphere of about 5% of the mean. The results for net solar radiation at the surface are also consistent with the Kalnay et al. estimate that the NCEP–NCAR net radiation at the surface is 5–8 W m^{-2} less than the climatological averages. Kalnay et al. (1996) suggest that the errors in upward shortwave radiation may be due to a systematic overestimate of the ocean surface albedo. However, the present results strongly suggest that this error is primarily attributable to errors in shortwave cloud forcing in the Tropics.

To further explore these two hypotheses, Eq. (2) is used to develop a simple regression equation of the form

$$\mathrm{SWCF} = \alpha f + \beta, \tag{4}$$

where α is the least squares best estimate of $(S_{\mathrm{clr}} - S_{\mathrm{cld}})$ and β is an intercept, which should be approximately zero. Figure 11 shows the point-by-point estimates of $(S_{\mathrm{clr}} - S_{\mathrm{cld}})$ using the NCEP–NCAR SWCF and f and, alternately, the ERBE SWCF and the ISCCP f. In both cases the β's equal zero within about ± 4 W m^{-2}. Figure 11 dramatically illustrates that the NCEP–NCAR $(S_{\mathrm{clr}} - S_{\mathrm{cld}})$ values are up to about twice the magnitude of the observational estimates over most of the Tropics. Furthermore, the differences between the two estimates are diminished at higher latitudes as are the differences between the NCEP–NCAR and ERBE annual mean SWCF (Fig. 3b). The differences in the Tropics represent a difference in shortwave cloud radiative forcing of up to about 0.9 W m^{-2} per percent of total cloud

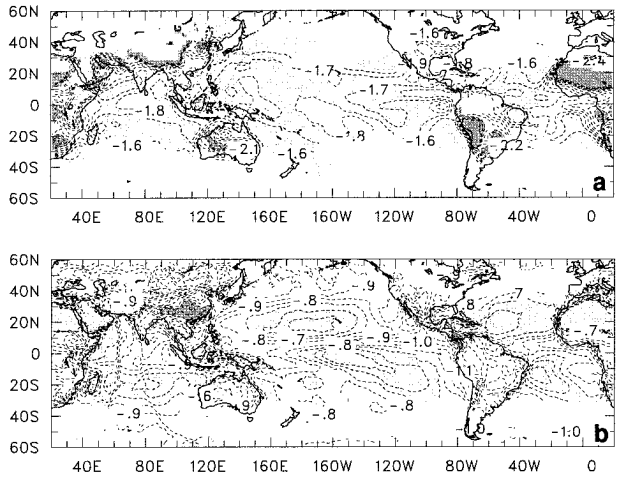

FIG. 11. Regression estimates of annual mean ($S_{clr} - S_{cld}$) from Eq. (4) for January 1985 through December 1988: (a) NCEP ($S_{clr} - S_{cld}$) [W m^{-2}(%)$^{-1}$] based upon NCEP–NCAR SWCF and *f*, and (b) observed ($S_{clr} - S_{cld}$) [W m^{-2}(%)$^{-1}$] based upon ERBS SWCF and ISCCP *f*. Values are plotted only for estimates corresponding to regression models that are significant at the 95% confidence level.

cover. For example, in the central equatorial Pacific with about 50% cloud cover this corresponds to excessive shortwave cloud radiative forcing of about 45 W m^{-2}, which is the approximate error displayed in Fig. 3b. Thus, these results are fully consistent with the hypothesis that the errors in shortwave fluxes are associated with excessively reflective clouds. They are inconsistent with the hypothesis that the errors are due to overestimates of surface albedos since the latter should lead to increases in S_{clr} and smaller magnitudes of α.

Seasonal variations (and the single analyzed interannual perturbation) of longwave cloud forcing are in generally good agreement with observations, and significant disagreements are usually reasonably well related to errors in high cloud amounts. The seasonal cycle of the NCEP–NCAR shortwave cloud forcing has a magnitude about 16% greater than that of the ERBS observations, although the variability of NCEP–NCAR total cloud amount is about 25% less than that of ISCCP. Errors in the seasonal variability of SWCF are apparently related to 1) a near-global specification of clouds that are too bright in the NCEP analysis model, 2) underestimation of the analyzed seasonal variability of total cloud amount, and perhaps 3) underestimates of the seasonal variability of tropical clear-sky fluxes. Patterns of differences between NCEP–NCAR and ERBE La Niña minus El Niño shortwave cloud forcing are largely attributable to errors in the location of anomalies in total cloud cover.

Several areas of future work are needed to more fully estimate the validity of the NCEP–NCAR radiation fields. First, there is currently no reliable global set of observations of net longwave radiation at the surface to be compared against the analyses. Without such observations it is impossible to fully assess the biases in the NCEP–NCAR products at either the surface or within the atmosphere. Second, uncertainties concerning the nature of the recorded NCEP–NCAR cloud fractions must be removed. If the current values do not emulate those used by the reanalysis radiative transfer model, then more representative values should be developed and distributed. Finally, in order to optimize the utility of the NCEP–NCAR shortwave radiation products, it would seem necessary for NCEP to further investigate the scattering properties of the NCEP model clouds and to adjust the analysis products to bring seasonal means into better agreement with observations. Alternatively, NCEP could make readily available the shortwave radiative properties of the model clouds so that individual investigators may better understand the biases and, possibly, make their own adjustments.

Acknowledgments. This work was supported by grants from the Climate Dynamics Division of the National Science Foundation and the Western Regional Center of the National Institute for Global Environmental Change. I especially thank Wesley Ebisuzaki at NCEP for his help. Mr. Jeremy Broestl helped make available the TOVS and SSM/I observations.

REFERENCES

Brunk, H. D., 1965: *An Introduction to Mathematical Statistics.* Blaisdell, 429 pp.

Cess, R. D., G. L. Potter, W. L. Gates, J.-J. Morcrette, and L. Corsetti, 1992: Comparison of general circulation models to Earth Radiation Budget Experiment data: Computation of clear-sky fluxes. *J. Geophys. Res.,* **97,** 20 421–20 426.

Diekmann, F. J., and G. L. Smith. 1989: Investigation of scene identification algorithms for radiation budget measurements. *J. Geophys. Res.,* **94,** 3395–3412.

Ferraro, R. R., F. Weng, N. C. Grody, and A. Basist. 1996: An eight-year (1987–1994) time series of rainfall, clouds, water vapor, snow cover, and sea ice derived from SSM/I measurements. *Bull. Amer. Meteor. Soc.,* **77,** 891–905.

Fu, R., A. Del Genio, and W. B. Rossow, 1990: Behavior of deep convective clouds in the tropical Pacific deduced from ISCCP radiances. *J. Climate,* **3,** 1129–1152.

Gates, W. L., 1992: AMIP: The Atmospheric Model Intercomparison Project. *Bull. Amer. Meteor. Soc.,* **73,** 1962–1970.

Greenwald, T. J., G. L. Stephens, T. H. Vonder Haar, and D. L. Jackson, 1993: A physical retrieval of cloud liquid water over the global oceans using Special Sensor Microwave/Imager (SSM/I) observations. *J. Geophys. Res.,* **98,** 18 471–18 488.

Harrison, E. F., P. Minnis, B. R. Barkstrom, V. Ramanathan, R. D. Cess, and G. G. Gibson, 1990: Seasonal variation of cloud radiative forcing derived from the Earth Radiation Budget Experiment. *J. Geophys. Res.,* **95,** 18 687–18 703.

Hartmann, D. L., and D. Doelling, 1991: On the net radiative effectiveness of clouds. *J. Geophys. Res.,* **96,** 869–891.

Houghton, J. T., L. G. Meira Filho, B. A. Callander, N. Harris, A. Kattenberg, and K. Maskel, Eds., 1996: *Climate Change 1995. The Science of Climate Change.* Cambridge University Press, 572 pp.

Kalnay E., and Coauthors, 1996: The NCEP/NCAR 40-year reanalysis project. *Bull. Amer. Meteor. Soc.,* **77,** 437–471.

Li, Z., and H. G. Leighton, 1993: Global climatologies of solar radiation budgets at the surface and in the atmosphere from 5 years of ERBE data. *J. Geophys. Res.,* **98,** 4919–4930.

Liao, X., W. B. Rossow, and D. Rind, 1995: Comparisons between SAGE II and ISCCP high-level clouds. 1. Global and zonal mean cloud amounts. *J. Geophys. Res.*, **100,** 1121–1135

Minnis, P., P. W. Heck, and D. F. Young, 1993: Inference of cirrus cloud properties using satellite-observed visible and infrared radiances. Part II: Verification of theoretical cirrus radiative properties. *J. Atmos. Sci.*, **50,** 1305–1322.

North, G. R., T. L. Bell, F. F. Cahalan, and F. J. Moeng, 1982: Sampling errors in estimation of empirical orthogonal functions. *Mon. Wea. Rev.*, **110,** 699–706.

Phillips, T. J., 1994: A summary documentation of the AMIP model. PCMDI Rep. 18, 343 pp. [Available from Program for Climate Model Diagnosis and Intercomparison, L-264, Lawrence Livermore National Laboratory, Livermore, CA 94550.]

——, 1996: Documentation of the AMIP models on the World Wide Web. *Bull. Amer. Meteor, Soc.*, **77,** 1191–1196.

Potter, G. L., J. M. Slingo, J.-J. Morcrete, and L. Corsetti, 1992: A modeling perspective on cloud radiative forcing. *J. Geophys. Res.*, **97,** 20 507–20 518.

Ramanathan, V., R. D. Cess, E. F. Harrison, P. Minnis, B. R. Barkstrom, E. Ahmad, and D. Hartmann, 1989: Cloud-radiative forcing and climate: Results from the Earth Radiation Budget Experiment. *Science*, **243,** 57–63.

Rossow, W. L., and R. A. Schiffer, 1991: ISCCP cloud data products. *Bull. Amer. Meteor. Soc.*, **72,** 2–21.

Susskind, J., P. Piraino, L. Rokke, L. Iredell, and A. Mehta, 1997: Characteristics of the TOVS Pathfinder Path A dataset. *Bull. Amer. Meteor. Soc.*, **78,** 1449–1472.

Weare, B. C., 1993: Multi-year statistics of selected variables from the ISCCP C2 data set. *Quart. J. Roy. Meteor. Soc.*, **119,** 795–808.

——, 1994: Interrelationships between cloud properties and sea surface temperatures on seasonal and interannual time scales. *J. Climate*, **7,** 248–260.

——, 1995a: Factors controlling ERBE longwave clear-sky and cloud forcing fluxes. *J. Climate*, **8,** 1889–1899.

——, 1995b: Evaluation of total cloudiness in AMIP during ENSO. *Proc. Int. Conf. on the Tropical Ocean Global Atmosphere (TOGA) Program*, Melbourne, Australia, World Meteor. Org., 628–634.

——, 1997: Climatic variability of cloud radiative forcing. *Quart. J. Roy. Meteor. Soc.*, **123,** 1055–1073.

——, and AMIP Modeling Groups, 1996: Evaluation of the zonal mean vertical structure of clouds and its variability in the Atmospheric Model Intercomparison Project. *J. Climate*, **9,** 3419–3431.

——, I. I. Mokhov, and AMIP Modeling Groups, 1995: Evaluation of total cloudiness and its variability in the atmospheric model intercomparison project. *J. Climate*, **8,** 2224–2238.

Wielicki, B. A., and J. A. Coakley Jr., 1981: Cloud retieval using infrared sounder data: Error analysis. *J. Appl. Meteor.*, **20,** 157–169.